

**Future of Alberta's Forests:
Impacts of Climate and Landscape Change
On Forest Resources**

Report to Alberta Innovates

April 2013

Report contributors listed alphabetically:

Axel Anderson

Water Program Lead, Foothills Research Institute
Hinton, AB, Canada T7V 1X6
Email: Axel.Anderson@gov.ab.ca

Allan L. Carroll

Department of Forest and Conservation Sciences
Forest Science Centre 2424 Mail Mall, University of British Columbia
Vancouver, BC, Canada V6T 1Z4
Email: Allan.Carroll@ubc.ca

Nicholas Coops

Canada Research Chair in Remote Sensing,
Integrated Remote Sensing Studio:
Forest Science Centre 2424 Mail Mall, University of British Columbia
Vancouver, BC, Canada V6T 1Z4
Email: nicholas.coops@ubc.ca

Vinod Mahat

Department of Renewable Resources, 211 Human Ecology Building
University of Alberta, Edmonton, AB, Canada T6G 2H1
Email: mahat@ualberta.ca

David R. Roberts

Department of Renewable Resources
751 General Services Building, University of Alberta
Edmonton, Alberta, Canada, T6G 2H1
Email: dr3@ualberta.ca

Scott E. Nielsen

Department of Renewable Resources
741 General Services Building, University of Alberta, Edmonton, Alberta, Canada T6G 2H1
Email: scott.nielsen@ales.ualberta.ca

Gordon B. Stenhouse

Foothills Research Institute
P.O. Box 6330, 1176 Switzer Dr.
Hinton, Alberta, Canada, T7V 1X6
gstenhouse@foothillsri.ca

Table of Contents

List of Tables	iv
List of Figures	vi
Executive Summary.....	1
Section 1: Future Climate Change and Forest Condition	3
1.1 Introduction	3
1.2 Materials and Methods.....	3
1.2.1 Climate	3
1.2.2 Species stress under changing climate	5
1.2.3 Disturbance: Fire	6
1.2.4 Disturbance: Harvest.....	8
1.3 Results.....	9
1.3.1 Disturbance Fire:.....	15
1.3.2 Disturbance Harvest:.....	17
1.4 Discussion.....	20
1.5 Acknowledgements.....	20
Section 2: Climate and Water	21
2.1 Introduction	21
2.2 Materials and Methods.....	24
2.2.1 Study Watershed and Data	24
2.2.2 Methodology.....	26
2.3 Results.....	32
2.3.1 Estimates of future monthly climate means.....	32
2.3.2 Disaggregation	35
2.3.3 HBV-EC Calibration.....	38
2.3.4 HBV-EC Application	40
2.3.5 Parameter Uncertainty	44
2.3.6 Forest Change	45
2.4 Discussion.....	47

2.5 Conclusion.....	50
2.6 Acknowledgements.....	50
Section 3: Climate and Plant Phenology	51
3.1 Introduction	51
3.2 Materials and Methods.....	54
3.2.1 Ecological niche models	54
3.2.2 Model Validation.....	56
3.2.3 Species habitat projections.....	57
3.2.4 Software	59
3.3 Results.....	59
3.3.1 Model Validation.....	59
3.3.2 Changes in species distributions.....	62
3.3.3 Changes in distribution of seasonal resources	65
3.4 Discussion.....	68
3.4.1 Climate change vulnerability of grizzly bear food items.....	68
3.4.2 Species of Concern.....	70
3.5 Conclusion.....	73
3.6 Acknowledgements.....	74
Section 4: The mountain pine beetle in novel pine forests: predicting impacts in a warming environment	75
4.1 Introduction	75
4.2 Methods.....	76
4.2.1 Climatic suitability.....	76
4.2.2 Landscape-scale projections of climatic suitability.....	78
4.2.3 Stand susceptibility	79
4.2.4 Future susceptibility.....	83
4.3 Results and Discussion	83
4.3.1 Climatic suitability.....	83
4.3.2 Stand susceptibility	85
4.3.3 Future susceptibility.....	88
4.4 Conclusions	90

Section 5: Environmental Stress and Susceptibility of Lodgepole Pine to Mountain Pine Beetle.....	104
5.1 Introduction	104
5.2 Methods and Materials.....	104
5.3 Results.....	105
5.4 Acknowledgements.....	109
Section 6: References.....	110

List of Tables

Table 1.1 List of all provided climate layers.....	9
Table 1.2 Accuracy of species models.....	12
Table 1.3 Yearly and total areas of disturbance	18
Table 2.4 Relative changes in watershed averaged mean monthly GCM projections of precipitation and air temperature for A1B, A2 and B1 scenarios for 2020s, 2050s and 2080s time periods.....	33
Table 2.5 Comparison of monthly statistics of daily precipitation, Tmax and Tmin observed at Coleman station during the period from 1965 to 1997 with synthetic data generated by LARS-WG. P-values calculated by the t-test and F-test for the monthly means and variances are shown. A probability of 0.05 or lower indicates a departure from the observations that is significant at the 5% level.....	37
Table 3.6 Area under the curve of the receiver operating characteristic (AUC) for all modelling methods, including the ensemble mean method which omits the SRE method (MEAN). The number of presence (Npres) and absence (Nabs) records in the training data sample p	61
Table 3.7 Summary of species' projected elevation and area changes within occupied grizzly bear habitat (Nielsen et al. 2009) for the 2080s period for two emissions scenarios: B1 (moderate warming) and A2 (aggressive warming). Median elevations (Elev) for the 1961-1990 period and the projected changes (Δ Elev) in 10th percentile (p10), median (p50), and 90th percentile (p90) elevation under each future climate scenario are listed, as are total range area (Area) and percent change in range area (Δ Area) for the 1961-1990 observed climate and the two 2080s climate projections. Percent stable area (Stable area) represents the proportion of the species' 1961-1990 range that is maintained in the projections for the 2080s. Trends of species' seasonal use by bears (Season) are based on findings of Munro et al. (2006).....	64
Table 4.1. Quantile regression model of the independent and interacting effects of tree diameter [measured at breast height (1.3m)], Q , an index of hybrid ancestry where 0 = lodgepole pine and 1 = jack pine (Cullingham et al. 2012), and effective latitude determined from Hopkins Bioclimatic Law (Hopkins 1920) on the number of mountain pine beetle offspring per female (r_{adj}) adjusted to account for post-sample mortality associated with lethal low temperatures (see text for details).....	91

Table 4.2. Area and percentage of climatically suitable (i.e. \geq moderate suitability), pine-dominant ($\geq 50\%$ of all tree species) stands with predicted low, moderate and high susceptibility (<i>S</i>) to attack by the mountain pine beetle (see text for details of susceptibility calculations). Climatic suitability was derived from the Safranyik model (Carroll et al. 2004). SRES scenarios (Nakićenović and Swart 2000) were run with the CGCM3 general circulation model (Scinocca et al. 2008), downscaled using climateWNA (Wang et al. 2006)	92
Table 4.2. Area and percentage of climatically suitable (i.e. \geq moderate suitability), pine-dominant ($\geq 50\%$ of all tree species) stands with predicted low, moderate and high susceptibility (<i>S</i>) to attack by the mountain pine beetle (see text for details of susceptibility calculations). Climatic suitability was derived from the Safranyik model (Carroll et al. 2004). SRES scenarios (Nakićenović and Swart 2000) were run with the CGCM3 general circulation model (Scinocca et al. 2008), downscaled using climateWNA (Wang et al. 2006)	92

List of Figures

Figure 1.1 Examples of generated climate data over Alberta. Annual Precipitation in 2020, 2080 and Maximum July temperature in 2020 and 2080 using 3 climate scenarios (A1B, A2 and B1)....	11
Figure 1.2 Spatial distribution of models	12
Figure 1.3 Example Map of Climatic suitability for Lodgepole Pine	14
Figure 1.4 Shows the fire regimes based on the LANDIS simulations	16
Figure 1.5 Quick look of the STAARCH disturbance detection results.....	17
Figure 1.6 left: temporal distribution of disturbed area for 2001-2011, right: monthly changes over the whole study period.	18
Figure 1.7 Overview of disturbances over the whole study area	19
Figure 2.8 Crowsnest Creek watershed with climate station, Coleman and gauging station, Crowsnest at Frank	25
Figure 2.9 Reference (observed) period daily climates aggregated to monthly scale and nine sets of future monthly climate means (precipitation, Tmax and Tmin) estimated for climate station, Coleman.....	35
Figure 2.10 Observed and LARS-WG generated monthly values of precipitation, T_{max} and T_{min}	36
Figure 2.11 Observed and HBV-EC simulated daily, monthly and annual streamflows during the calibration period from 1965 to 1997. HBV-EC is driven by the daily climates observed at Coleman station.....	39
Figure 2.12 Same as figure 4, but in this case HBV-EC is driven by the LARS-WG generated daily climates.....	41
Figure 2.13 HBV-EC simulated mean monthly and mean annual streamflows for the reference and nine future periods (for three different scenarios: A1B, A2 and B1and for three different time periods: 2020s, 2050s and 2080s) at the watershed outlet at Crowsnest at Frank.	43
Figure 2.14 HBV-EC simulated watershed averaged mean monthly snow water equivalent (SWE) and mean monthly evapotranspiration for the reference and future periods	44
Figure 2.15 Ensemble of relative changes in mean monthly streamflows in different future periods compared to reference period streamflow, and mean of the ensemble.....	45
Figure 2.16 Ensemble and mean values of relative changes in mean monthly streamflows: a) due to forest removal b) due to climate change in 2080s in A2 scenario and c) due to combined forest removal and climate change in 2080s in A2 scenario. Figure 9d shows the ensemble mean to compare the relative changes in mean monthly streamflows due to forest removal, due to climate change in 2080s in A2 scenario and due to combined forest removal and climate change in 2080s in A2 scenario.....	46

Figure 3.17 Location of the study area in the western Canadian Rocky Mountains, showing topographic profile. Present-day grizzly bear range for the southern Canadian Rockies (Nielsen et al. 2009) is outlined in blue	54
Figure 3.18 Boxplot showing model accuracy as measured by the area under the curve of the receiver operating characteristic (AUC) for each species and all modelling methods, including the ensemble mean method (MEAN), the AUCs for which are shown as black dots. A complete table of AUC values for each species within each method and number of observed presences and absences is provided in Table 3.2.....	60
Figure 3.19 Standard deviations of the ensemble mean species projections of probability of presence, averaged across all species, as a measure of model uncertainty. The black outline represents modern grizzly bear habitat in the southern Canadian Rockies (Nielsen et al. 2009).....	62
Figure 3.20 Maps showing the change from the 1961-1990 period in number of species projected present for the A2 scenario of the 2080s period. Changes are shown by season for (a) spring, (b) summer, and (c) autumn, with the seasonally-important bear food source species (see Table 1). (d) Changes in counts of all 17 species considered (all seasons together), is also shown. Areas of unsuitable range (agriculture, rock, ice, water, etc.) are masked in white. The range of present-day grizzly bear habitat in the southern Canadian Rockies is shown as a black outline. Maps of absolute counts of species are shown in Figure 3.5.....	66
Figure 3.21 Maps showing counts of projected species for the 1961-1990 period and for the B1 and A2 scenarios for the 2080s period for (a) all species, as well as species identified as seasonally important for bears in (b) the spring, (c) the summer, and (d) the autumn. Areas of unsuitable range (agriculture, rock, ice, water, etc.) are masked in white. Present-day grizzly bear habitat in the southern Canadian Rockies is shown as a red outline.....	67
Figure 4.1 Location of r-value sample sites in Alberta from 2006 to 2011. Sampling was conducted by Alberta Environment and Sustainable Resources Development.....	106
Figure 4.2 Distributions of pine-dominant ($\geq 50\%$ of tree species) stands indicating their climatic suitability during recent decades for the mountain pine beetle. Climatic suitability classes were derived from the Safranyik model of climatic suitability (Carroll et al. 2004) and mean conditions for 1981-2010	1075
Figure 4.3 Distributions of pine-dominant ($\geq 50\%$ of tree species) stands indicating their future climatic suitability for the mountain pine beetle derived from the Safranyik model of climatic suitability (Carroll et al. 2004) and 3 climate change scenarios [Special Report on Emissions Scenarios (SRES)] run with the CGCM3 general circulation model (Scinocca et al. 2008) and downscaled using climateWNA (Wang et al. 2006). Scenario (A2) = no change in the rate of greenhouse gas emissions; Scenario B1= emissions declining by 2040 to half of the current rate by 2100; scenario A1B = intermediate emissions between A2 and B1 (Nakićenović and Swart 2000).....	1086

- Figure 4.4 Distributions of pine-dominant ($\geq 50\%$ of tree species) stands indicating their future climatic suitability for the mountain pine beetle derived from the Safranyik model of climatic suitability (Carroll et al. 2004) and the A2 climate change scenario (Nakićenović and Swart 2000) run with the CGCM3 general circulation model (Scinocca et al. 2008) and downscaled using the Canadian Regional Climate Model (Caya et al. 1995)..... 109
- Figure 4.5 Scatterplots and quantile regression fits examining the relationship between tree diameter [measured at breast height (1.3m)] and the number of mountain pine beetle offspring per female (r), adjusted to account for post-sample mortality associated with lethal low temperatures (see text for details). Where significant, quantile regression lines (i.e. 10th, 25th, 75th, and 90th percentiles) are superimposed on the plot in gray, the median fit in solid blue, and the least squares estimate of the conditional mean function as the dashed red line. Scatterplots are presented along axes denoting the significant interaction between Q , an index of hybrid ancestry where 0 = lodgepole pine and 1 = jack pine (Cullingham et al. 2012), and effective latitude determined from Hopkins Bioclimatic Law (Hopkins 1920). Sampling locations representing combinations of effective latitudes >64.5 and Q values from 0.10 – 0.20 and >0.20 did not exist, and therefore scatterplots are not shown. See text for details. 1098
- Figure 4.6 Current distribution of climatically suitable (i.e. \geq moderate suitability), pine-dominant ($\geq 50\%$ of tree species) stands indicating their susceptibility to attack by the mountain pine beetle (see text for details of susceptibility calculations). Climatic suitability was derived from the Safranyik model (Carroll et al. 2004) and mean conditions for 1981-2010 109
- Figure 4.7 Future distributions of climatically suitable (i.e. \geq moderate suitability), pine-dominant ($\geq 50\%$ of tree species) stands indicating their predicted susceptibility to attack by the mountain pine beetle (see text for details of susceptibility calculations). Climatic suitability was derived from the Safranyik model (Carroll et al. 2004) and the A2 climate change scenario (Nakićenović and Swart 2000) run with the CGCM3 general circulation model (Scinocca et al. 2008), downscaled using climateWNA (Wang et al. 2006) 100
- Figure 4.8 Future distributions of climatically suitable (i.e. \geq moderate suitability), pine-dominant ($\geq 50\%$ of tree species) stands indicating their predicted susceptibility to attack by the mountain pine beetle (see text for details of susceptibility calculations). Climatic suitability was derived from the Safranyik model (Carroll et al. 2004) and the A1B climate change scenario (Nakićenović and Swart 2000) run with the CGCM3 general circulation model (Scinocca et al. 2008), downscaled using climateWNA (Wang et al. 2006) 101
- Figure 4.9 Future distributions of climatically suitable (i.e. \geq moderate suitability), pine-dominant ($\geq 50\%$ of tree species) stands indicating their predicted susceptibility to attack by the mountain pine beetle (see text for details of susceptibility calculations). Climatic suitability was derived from the Safranyik model (Carroll et al. 2004) and the B1 climate change scenario (Nakićenović and Swart 2000) run with the CGCM3 general circulation model (Scinocca et al. 2008), downscaled using climateWNA (Wang et al. 2006) 102

Figure 4.10 Future distributions of climatically suitable (i.e. \geq moderate suitability), pine-dominant (\geq 50% of tree species) stands indicating their predicted susceptibility to attack by the mountain pine beetle (see text for details of susceptibility calculations). Climatic suitability was derived from the Safranyik model (Carroll et al. 2004) and the A2 climate change scenario (Nakićenović and Swart 2000) run with the CGCM3 general circulation model (Scinocca et al. 2008), downscaled using the Canadian Regional Climate Model (Caya et al. 1995)	103
Figure 5.22: Location of plots with R values available across Alberta	106
Figure 5.23: Long term distribution of Lodgepole pine as modelled using methods discribed in section 1.....	107
Figure 5.24: Predicted stress of Lodgepole pine as modelled using methods discribed in section 1	108
Figure 5.25: Relationship between years unsuitable for lodgepole pine between 2005 and 2009, and adjusted r values.....	109

Executive Summary

Future climate condition across Alberta will likely produce a range of impacts on forest condition and health including impacts on vegetation condition, forest hydrology, insect infestation and phenology. In this study, the overall impacts of future climate change are examined across these broad topic areas.

To do so, first a suite of climate layers were developed over Alberta, including both past and future climate conditions. These layers were provided to the other researchers on the project provided a base for the presented studies. Forest disturbance was also mapped and analyzed using a remote sensing approach which incorporated both high and low spatial resolution data.

A second study evaluated the impacts of climate and forest changes on streamflow in the upper parts of the Oldman in Southern Alberta using a conceptual hydrological model, HBV-EC in combination with a stochastic weather generator (LARS-WG) driven by GCM output climate data. Three climate change scenarios (A1B, A2 and B1) are selected to cover the range of possible future climate conditions (2020s, 2050s, and 2080s). GCM projected less than 10 % increase in precipitation in winter and about same amount of precipitation decrease in summer. These changes in projected precipitation resulted in up to 200% (9.3 mm) increase in winter streamflow in February and up to 63% (31.2 mm) decrease in summer flow in June.

A third study investigated climate change vulnerability for *Ursus arctos* (grizzly bears) in the southern Canadian Rocky Mountains using projected changes to 17 of the most commonly consumed plant food items. We used presence-absence information from 7,088 field plots to estimate ecological niches and to project changes in future distributions in each species. Model projections indicated idiosyncratic responses among food items. Many food items persisted or even increased, although several species were found to be vulnerable based on declines or geographic shifts in suitable habitat including

Hedysarum alpinum (alpine sweet vetch), a critical spring and autumn root-digging resource when little else is available. Potential habitat loss was also identified for three fruiting species of lower importance to bears: *Empetrum nigrum* (crowberry), *Vaccinium scoparium* (grouseberry) and *Fragaria virginiana* (wild strawberry). A general trend towards uphill migration of bear foods may result in higher vulnerability to bear populations at low elevations which are also those that are most likely to have human-bear conflict problems.

In a fourth study, the important question regarding population dynamics of the mountain pine beetle in novel habitats and the impact of a warming environment were examined. Using model projections for climate, climatically suitable habitats to the beetle based on a range of greenhouse gas emissions scenarios for the Foothills region of Alberta were determined. Projections of climatic suitability were combined with a model of stand susceptibility for mountain pine beetle derived from empirical measures of beetle productivity in novel habitats, to project the distribution and abundance of climatically suitable and susceptible pine stands into the future. Despite the historic unsuitability of the Foothills region to the mountain pine beetle due to the adverse effects of climate, even under the most conservative climate change scenario the vast majority of the pine-dominant stands in the area are projected to become highly suitable and susceptible by the middle of this century.

In the fifth and final study, links between climate, tree species stress, and infestation by the mountain pine beetle (*Dendroctonus ponderosae*) are examined. Together with stand-level parameters (e.g. species, density, age, etc.) recorded during the sampling, variables derived from detailed stand-level vegetation resource inventory dataset, and weather data, r-values can be used to predict the size of an emerging MPB population.

Section 1: Future Climate Change and Forest Condition

Contributing Author: Nicholas Coops

1.1 Introduction

Capturing future climate variation and disturbance for ongoing characterization of the landscape is necessary for future sustainable forest management and biodiversity conservation. By mapping landscape disturbance we will gain insights on what changes, by type and location, are occurring over the study area and how forest resources are impacted by change. Characterization of habitat recovery post-disturbance is also important for this long-term monitoring and modeling program. These drivers of change include climate, modified fire regimes, and anthropogenic changes such as variable harvesting regimes, and exploration activities for oil and gas. The development of comprehensive management and conservation strategies therefore requires explicit modelling of these drivers, including various levels of spatial data integration to produce meaningful data layers from disturbance, phenology, and climate scenarios inputs. When combined these layers will enable the development of a range of scenarios each producing a future landscape from which three focal forest resources (water, plant phenology, and mountain pine beetle) will be evaluated.

1.2 Materials and Methods

1.2.1 Climate

Mean monthly climate spatial surfaces are generated using ClimateWNA, which downscales precipitation and temperature data generated at 2 - 4 km by PRISM (Wang et al. 2006) Parameter-elevation Regressions on Independent Slopes Model, (Daly et al. 2002) to 1 km. A 90m-Digital Elevation Model (DEM), obtained from the Shuttle Radar Topography Mission (SRTM), was resampled to 1 km to provide the required elevation data at the same resolution as the climatic data. The downscaling is achieved through a combination of bilinear

interpolation and elevation adjustment. We will compute monthly coverages of precipitation, minimum and maximum temperature from 1950 to 2010.

To simulate conditions under a future projected climate, we will utilize the Special Report on Emission Scenarios (SRES) climate scenarios developed by the Intergovernmental Panel on Climate Change (IPCC) Fourth Assessment Report, AR4 (Nakicenovik and Swart 2000; IPCC 2007). Three climate scenarios were produced: “a business as usual” scenario (A2), a scenario (B1) that assumes current emissions rates will remain steady until around 2040, and then slowly drop to about half of the current rate by the end of the century and a third in between scenario (A1B). Monthly climate layers were produced for three standard 30-year periods, the 2020`s (2011-2040), 2050`s (2041 – 2070) and the 2080`s (2071 – 2100).

A number of secondary climate layers were also produced. Mean monthly atmospheric VPD for daylight periods was calculated by assuming that the water vapor concentrations present throughout the day would be equivalent to that held at the mean minimum temperature (Kimball et al 1997). The maximum VPD was calculated each month as the difference between the saturated vapor pressure at the mean maximum and minimum temperatures. Mean daytime VPD was calculated as half of the maximum value (Waring 2000).

The number of days per month with subfreezing temperatures (< -2 C) was estimated from empirical equations with mean minimum temperature (Coops et al 1998), such that:

$$\text{Number of Frost days} = 11.62 - (T_{min} * 1.57)$$

Monthly estimates of total incoming short-wave radiation were calculated using a modeling approach detailed by Coops et al (2000) where the potential radiation reaching any spot is first calculated and then reduced, based on the clarity (transmissivity) of the atmosphere (Goldberg et al 1979; Bristow and Campbell 1984; Hungerford et al 1989). Changes in the atmospheric transmissivity are mirrored in temperature extremes. With the digital elevation model, we adjusted for differences in slope, aspect, and elevation as well as for variations in the fraction of diffuse and direct solar beam radiation (Garnier and Ohmura 1968; Buffo et al 1972; Swift 1976; Hungerford et al 1989). The modeling approach, when compared with direct measurements, predicted both the direct and diffuse components of mean monthly incoming radiation with 93 - 99% accuracy on flat surfaces, and on sloping terrain accounted for >87% of the observed variation with a mean error < 2 MJ m⁻² day⁻¹ (Coops et al 2000).

1.2.2 Species stress under changing climate

In order to obtain information on changes in forest species growth, and future species distribution we will apply the 3-PG simply physiological model (Landsberg and Waring 1997) which contains a number of simplifying assumptions that have emerged from studies conducted over a wide range of forests types and include the use of monthly climate data (rather than daily or annual) with little loss in the accuracy of model predictions. Each month, the most limiting climatic variable on photosynthesis is selected, based on departure from conditions that are defined as optimum (expressed as unity) or completely limited (expressed as zero) for a particular species or genotype. The ratio of actual/potential photosynthesis decreases in proportion to the reduction in the most limiting environmental factor. The fraction

of production not allocated to roots is partitioned among foliage, stem and branches based on allometric relationships and knowledge of annual leaf turnover (Landsberg et al. 2003).

To assess levels of stress in the modeled tree species we first assessed the extent that suboptimal temperature, frost, drought, and humidity deficits affect photosynthesis and growth of the species across Alberta with the 3PG process-based model. We then entered the same set of climatic variables into a decision- tree model, which creates a suite of rules that differentially rank the variables, to provide a basis for predicting presence or absence of the species under current climatic conditions. The derived decision-tree model successfully predicted weighted presence and absence recorded on field survey plots with an accuracy of ~70%. Once the models for each species were developed we ran the species models annually using the data generated above for the period between 1976 and 2006, across the region. Using an approach described in Coops and Waring (2011) and then established which tree species are deemed resilient to recent changes in climate (assuming < 50% of years were designed as climatically inside the previously defined limits) and those species that are more vulnerable.

1.2.3 Disturbance: Fire

In order to capture past and future landscape patterns due to fire and harvesting disturbance regimes we will use the LANDIS modelling framework (Mladenoff and He, 1999, Mladenoff et al., 1996). LANDIS is a landscape scale model which works across a range of spatial and temporal scales. Regions can be defined within the study area which have varying responses to a range of disturbances such as fire, harvesting, and wind as well as forest dynamics such as succession. LANDIS can be parameterised for a range of both overstory and understory species, and has a capacity to incorporate future climate with respect to fire fuel development and

changes in future forest growth patterns. LANDIS is a spatially explicit, stochastic, raster-based model which each spatial cell is tracked with respect to presence / absence of species cohorts as well as fire and fuel characteristics.

The model has been applied to a large number of ecosystems around the world, and has active team of developers who are adding and refining modules based on individual model applications. The LANDIS fire module was developed by He and Mladenoff (1999) and predicts the mean fire return interval as a probabilistic function based on land cover, the number of years since a previous fire, and the fire return interval of the landscape. Fire size is defined by integrating random factors with the mean fire size and information on the smallest, mean and largest fire size expected. As a result fire disturbances are stochastic with smaller fires more likely to occur than larger ones as is typically observed. The severity of fire is based on fuel accumulation and time since previous fire as well as species fire resilience.

Our approach to using the LANDIS fire modules was as follows:

In order to parameterize the fire module within LANDIS we will utilise data from the August 20, 2008 release of the Canadian National Fire Database (NFDB). Locations of fire will be selected within increasing buffers centred over the study area and for each buffer distance fire events will be separated into three decades: 1977-1986; 1987-1996; and 1997-2006. The maximum, minimum, and mean fire size will then be calculated for each decade and the average decadal fire density determined by dividing the number of points within each decadal category by the total area. Fire returns frequency within the study area will be determined from the literature.

Once the predicted fire patterns match those patterns observed in the NFDB and by the MODIS hot spot datasets we will predict the future role of fire on the study area by developing a set of fire scenarios. A base level set of scenarios will be developed as part of this project including representing fire regimes over the 30 years, as well as an increasing and a decreasing scenario based on historical high and low patterns of fire in the region. Fire frequency will also vary based on future forest state, with available forest fuel also strongly linked to stand age. It is anticipated that an additional project may be needed in order that the basic fire module, once correctly calibrated, be linked to the climate change scenarios, where forest fuel will vary based on changes in temperature and precipitation regimes. This additional component of the project is under discussion by the research team.

1.2.4 Disturbance: Harvest

Habitat structure and the distribution of wildlife species, such as grizzly bears, can be strongly influenced by the spatial and temporal distribution of vegetation structure and by vegetation phenology. To date we have developed a new approach to predict landscape disturbances post 2000 using a fusion of high spatial resolution Landsat imagery with high temporal resolution imagery such as Moderate Resolution Imaging Spectroradiometer (MODIS). The algorithm, Spatial Temporal Adaptive Algorithm for mapping Reflectance Change (STAARCH) (Hilker et al. 2009), was developed as an extended version of STARFM to allow the detection of disturbance events at spatial scales smaller than that of a MODIS pixel, through the generation of a spatial change mask derived from Landsat and an image sequence recording the temporal evolution of disturbance events (based on MODIS). STAARCH was then applied over the entire grizzly bear study area (6 million ha) by Gaulton et al (2011) from 2001 to 2008 who found the majority of

individual disturbance events were small in terms of area (mean patch size of 3.84 ha, standard deviation of 7.2 ha) with the most covering between 1 and 5 ha. A smaller number of larger disturbance events also occurred such as fire, with the largest covering an area of 1028 ha over the 8 year period.

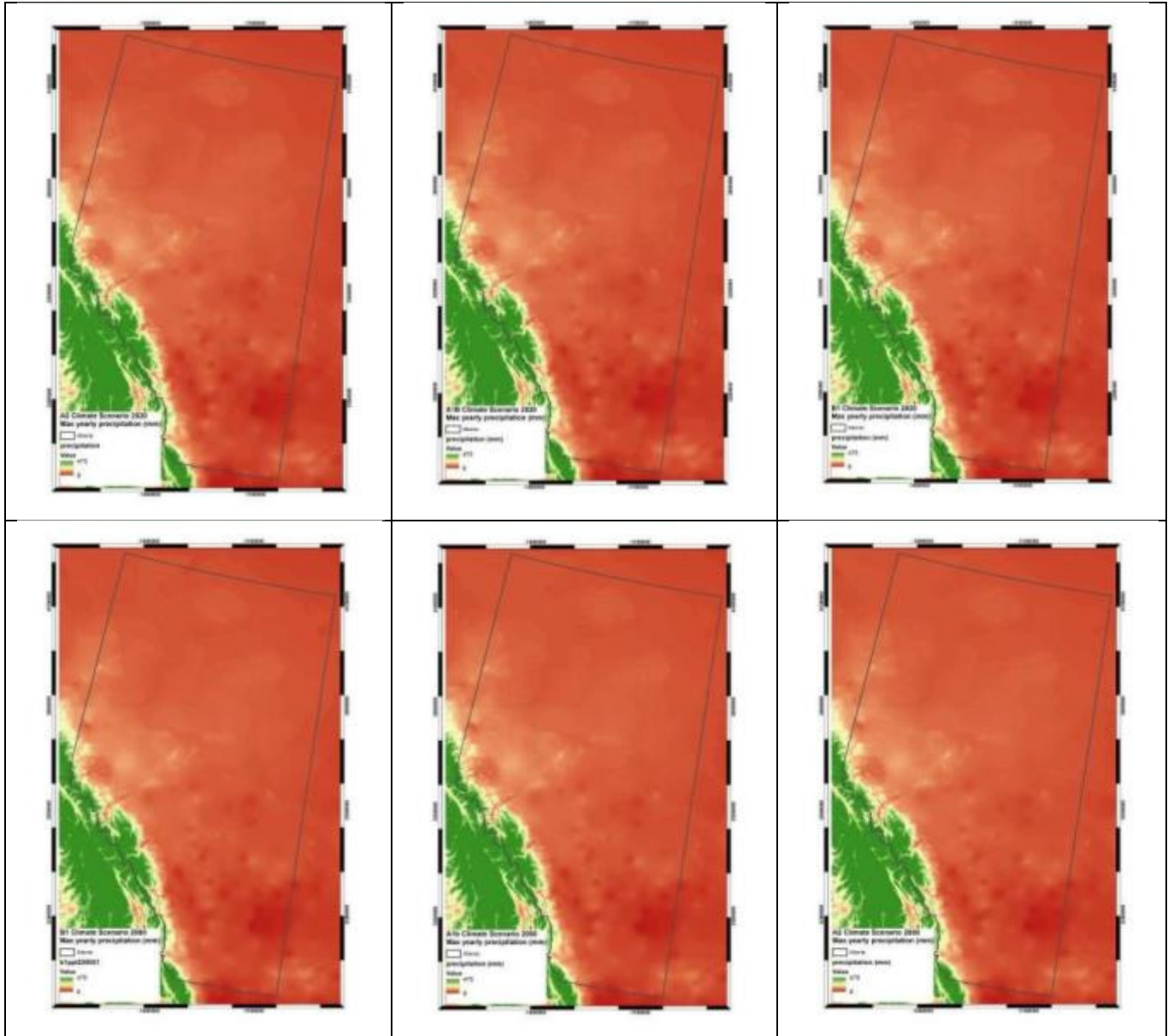
1.3 Results

All provided climate layers are listed in Table 1.1.

Table 1.1 List of all provided climate layers.

Climate Data Characteristics	
Spatial Resolution	1 x 1 km
Geographic Region	Alberta
Software	Climate WNA (Wang et al 2009)
Time interval	Monthly
Date Range	1950 – 2009, 2020, 2050 and 2080
Climate Change Simulations	Assessment Report AR4
Circulation Model	Canadian Climate Centre's Modelling and Analysis (CCCma) 3 rd generation GCM (CGCM3)
Climate Data Generated	Maximum Temperature (°C)
	Minimum Temperature (°C)
	Precipitation (mm)
Derived Climate Data	Vapour Pressure Deficit (Hpa)
	Total Incoming Radiation (MJ m ² Day)
	Number of Frost Days (days)
Data Format	ARCINFO ESRI GRID FORMAT
	Export Float Format

Examples of generated climate data over Alberta, including Precipitation and Maximum July temperature are shown in Figure 1.1 and 1.2.



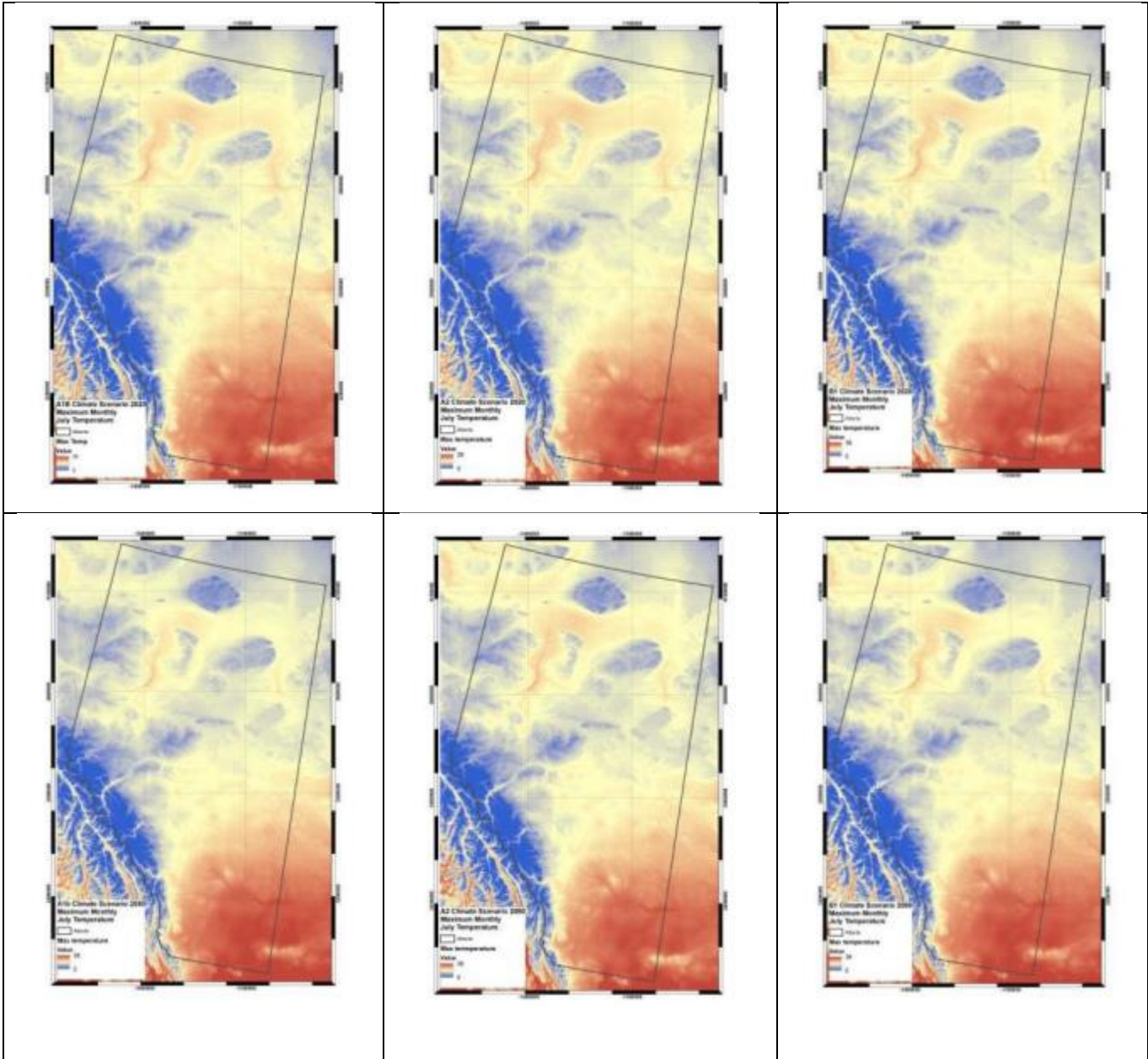


Figure 1.1 Examples of generated climate data over Alberta. Annual Precipitation in 2020, 2080 and Maximum July temperature in 2020 and 2080 using 3 climate scenarios (A1B, A2 and B1).

Table 1.2 Accuracy of species models.

Species	Presence Accuracy (%)	Absence Accuracy (%)	Overall average (%)	κ
Lodgepole pine	68	78	70	0.6258
Douglas fir	74	80	78	0.5985
Subalpine fir	95	62	79	0.8555
Engelmann spruce	84	72	78	0.8872
Whitebark pine	91	81	86	0.8053
Quaking aspen	82	71	77	0.8947
Rocky mountain juniper	90	82	86	0.7837

Spatial distributions of the models are shown in Figure 1.2

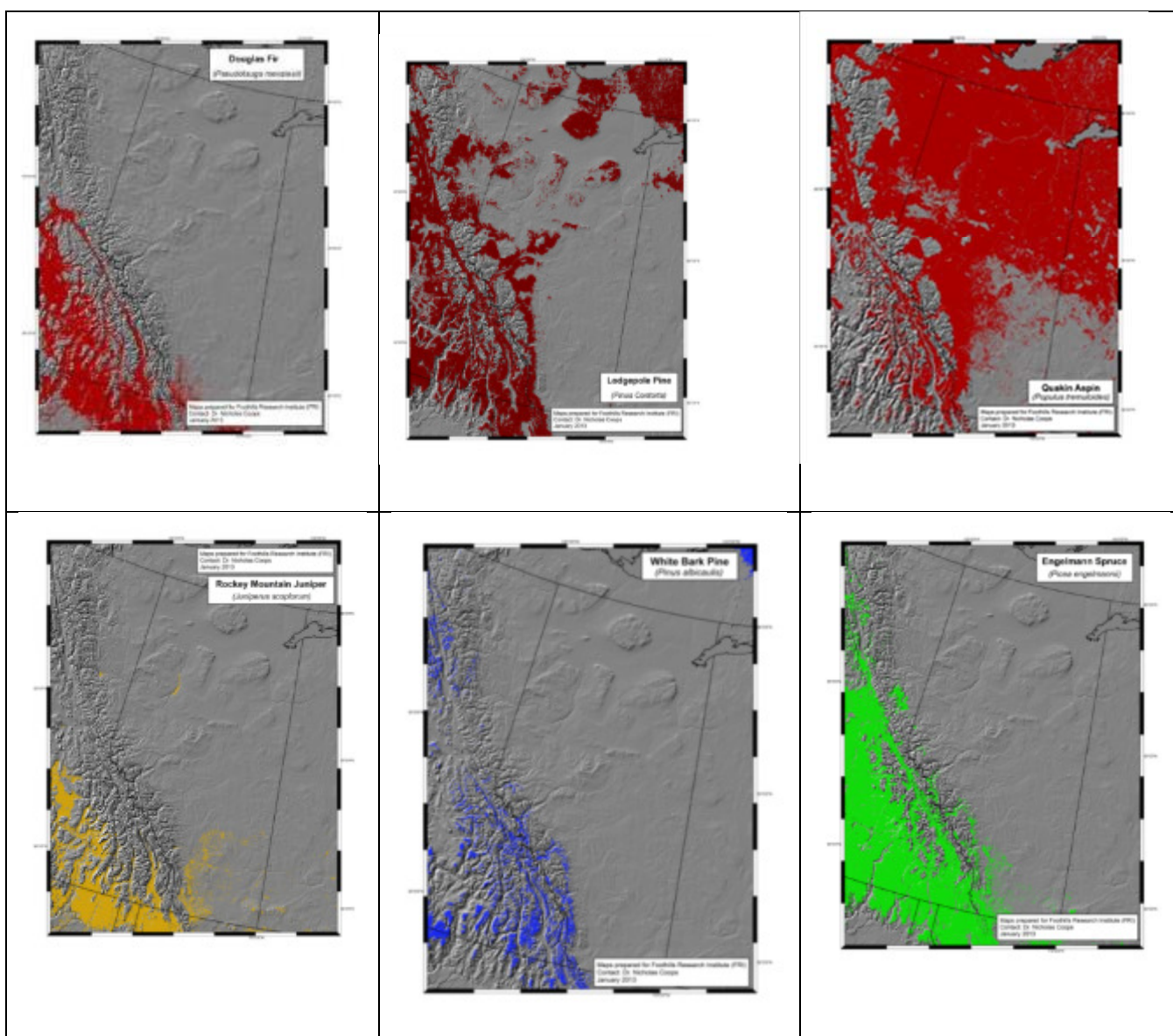


Figure 1.2 Spatial distribution of models.

We applied the decision tree models to assess the number of years between 1976 and 2006 when climatic conditions during 1 or more years departed sufficiently from the calibration period to predict the absence of a species within its previously modeled range. Areas where the climatic conditions remained suitable from 1976 and 2006 are shown in red whereas locations where the species appears more vulnerable are depicted in green, yellow, and blue colors, indicative of progressively less favorable conditions. In the case of lodgepole pine, the species remained well adapted to the climate variability throughout most of Alberta, becoming more vulnerable in the central regions on the eastern slopes of the Rocky Mountains.

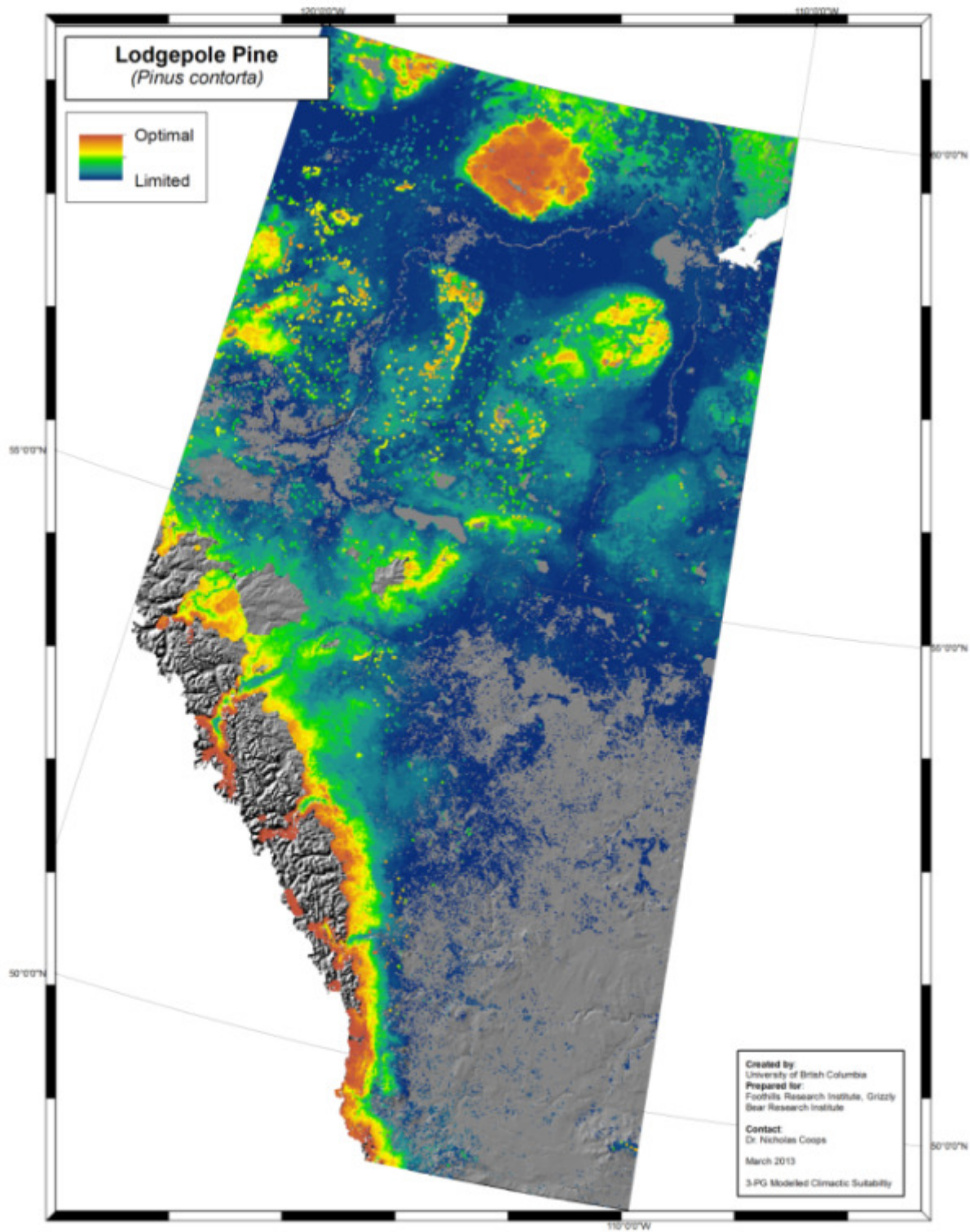


Figure 1.3 Example Map of Climatic suitability for Lodgepole Pine.

1.3.1 Disturbance Fire:

For the modeling of fire disturbances, we utilize the latest Landscape Disturbance and Succession Model, LANDIS-II v6.0 Release Candidate 3, using a powerful desktop workstation to run the simulations across an area 25,223,628 hectares in size at 300-meter resolution – a task recently made possible by memory utilization improvements to the model.

For the included LANDIS-II simulation results, we projected the future effects of the continuation of three different historical 30-year patterns in forest fire distribution (e.g., fire frequency, mean fire size, maximum fire size, minimum fire size, annual area burned) and climate change (maximum temperature, minimum temperature, and precipitation). We used novel methods to parameterize the model, including a method utilizing soils and climate data currently available Canada-wide to parameterize the Tree and Climate Assessment Germination model, TACA-GEM, to model changing species establishment within LANDIS-II. We conducted a rules-based classification of a recent bioclimatic envelope model, or species distribution model, that uses ClimateWNA (Wang et al. 2012) to estimate species distributions based on their realized niche (Gray and Hamann 2013), using the same 30-year climate average data, kept static as a control variable.

The age class distribution of the species at each site was also held as constant to exhibit the effects of inter-regional heterogeneity in changing landscape patterns due to the climate and fire regime parameterization. Species life history attribute data for 13 primary tree species in the Phase 7 Study Area was gathered from primary source peer-reviewed literature where possible and secondary source published tree species compendiums. The ecological regions of the study area are based on the biogeoclimatic Natural Subregions of Alberta (Alberta ESRD

2005), which was deemed an appropriate initial approximation and scale for species establishment and forest fire statistical distributions.

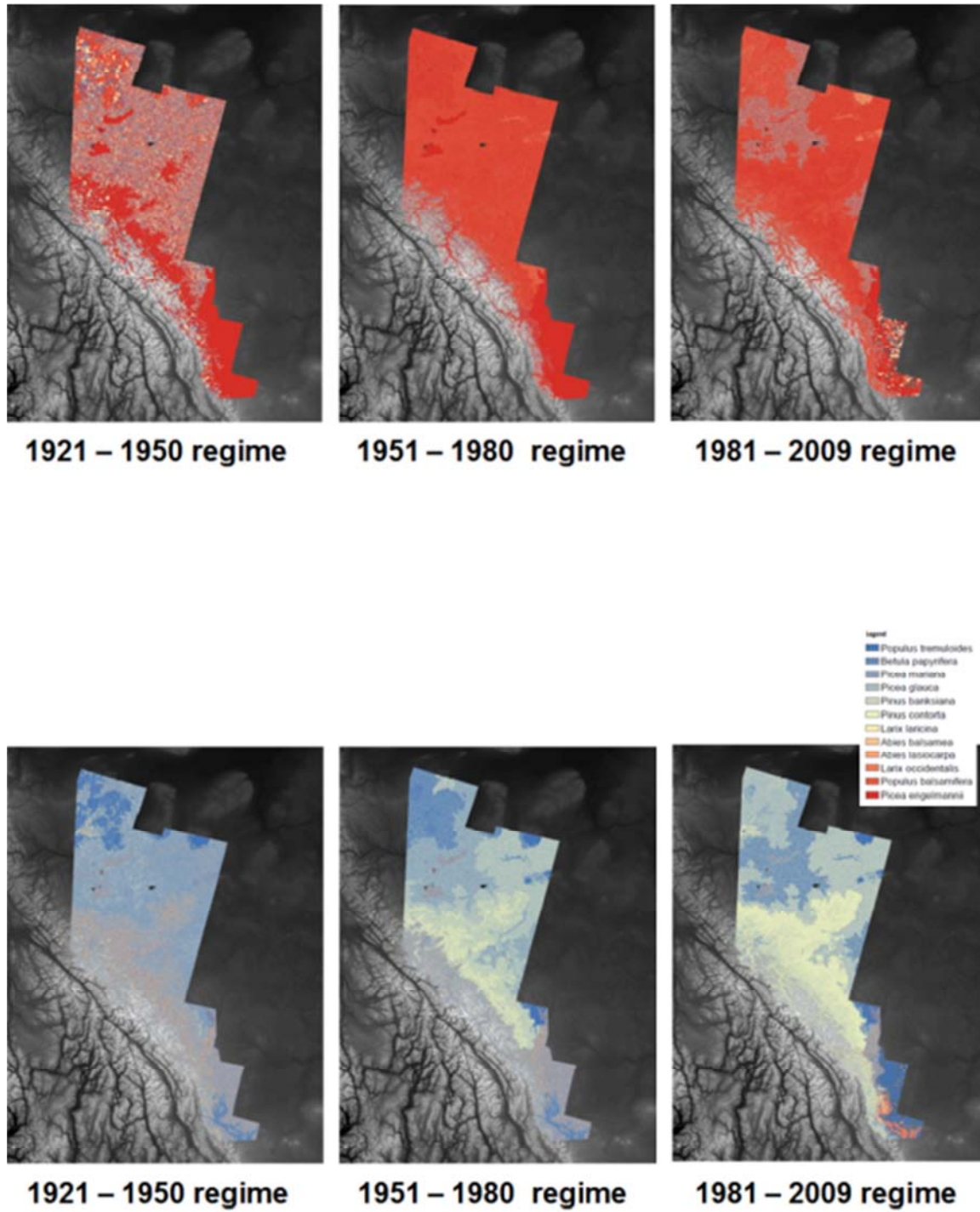


Figure 1.4 Shows the fire regimes based on the LANDIS simulations.

1.3.2 Disturbance Harvest:

The STAARCH Change product contains polygons over the area showing the changed areas and the detected date of change. Fig 1.5 shows two subsets of the study area as a quick look of the results. An overview of the entire study area is shown in Figure 1.7.

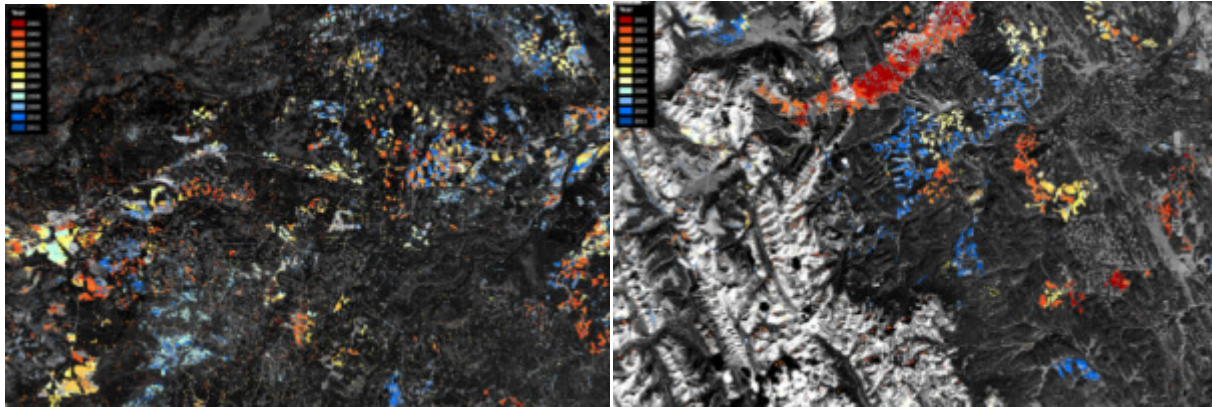


Figure 1.5 Quick look of the STAARCH disturbance detection results.

In each of the studied years between 40000 and 90000 ha of land was detected as change, note that 2001 and 2011 were only half years and thus show lower numbers. The sum of the changed area over this decade of change detection is 5558 square kilometer, which is approximately 4% of the study area (Table 1.3)

Table 1.3 Yearly and total areas of disturbance.

Year	Changed Area [ha]	Percentage of RSF Area
2001	7343	0.06%
2002	39818	0.30%
2003	87898	0.67%
2004	40421	0.31%
2005	47147	0.36%
2006	41258	0.31%
2007	46988	0.36%
2008	61905	0.47%
2009	73161	0.56%
2010	72358	0.55%
2011	37496	0.29%
Total	555794	4.23%

The temporal patterns of harvesting during the whole detection period and monthly within all years is shown in Fig 1.6. The patterns show a concentration of harvesting in the spring and autumn seasons. It has to be noted that winter harvesting cannot be reliably detected because of snow and any harvesting during that period is thus assigned to the following spring.

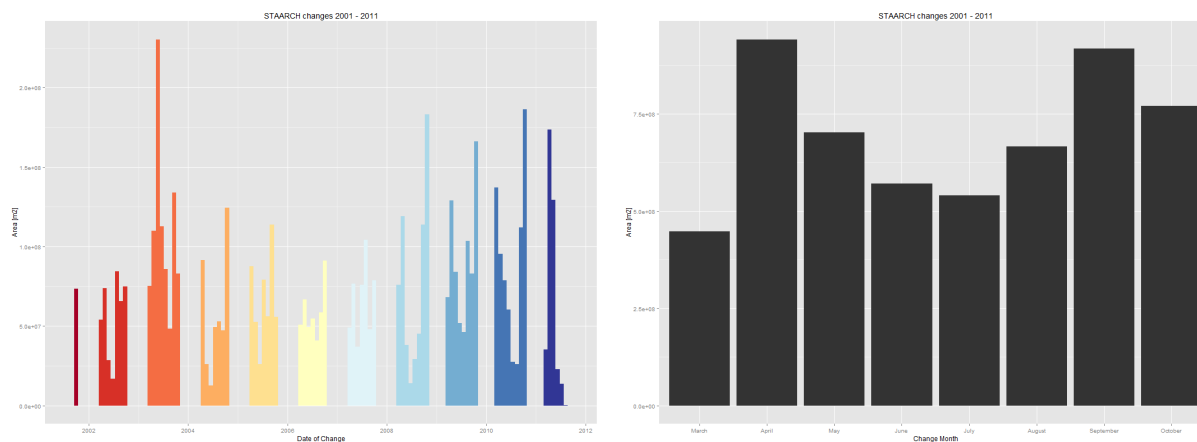


Figure 1.6 left: temporal distribution of disturbed area for 2001-2011, right: monthly changes over the whole study period.

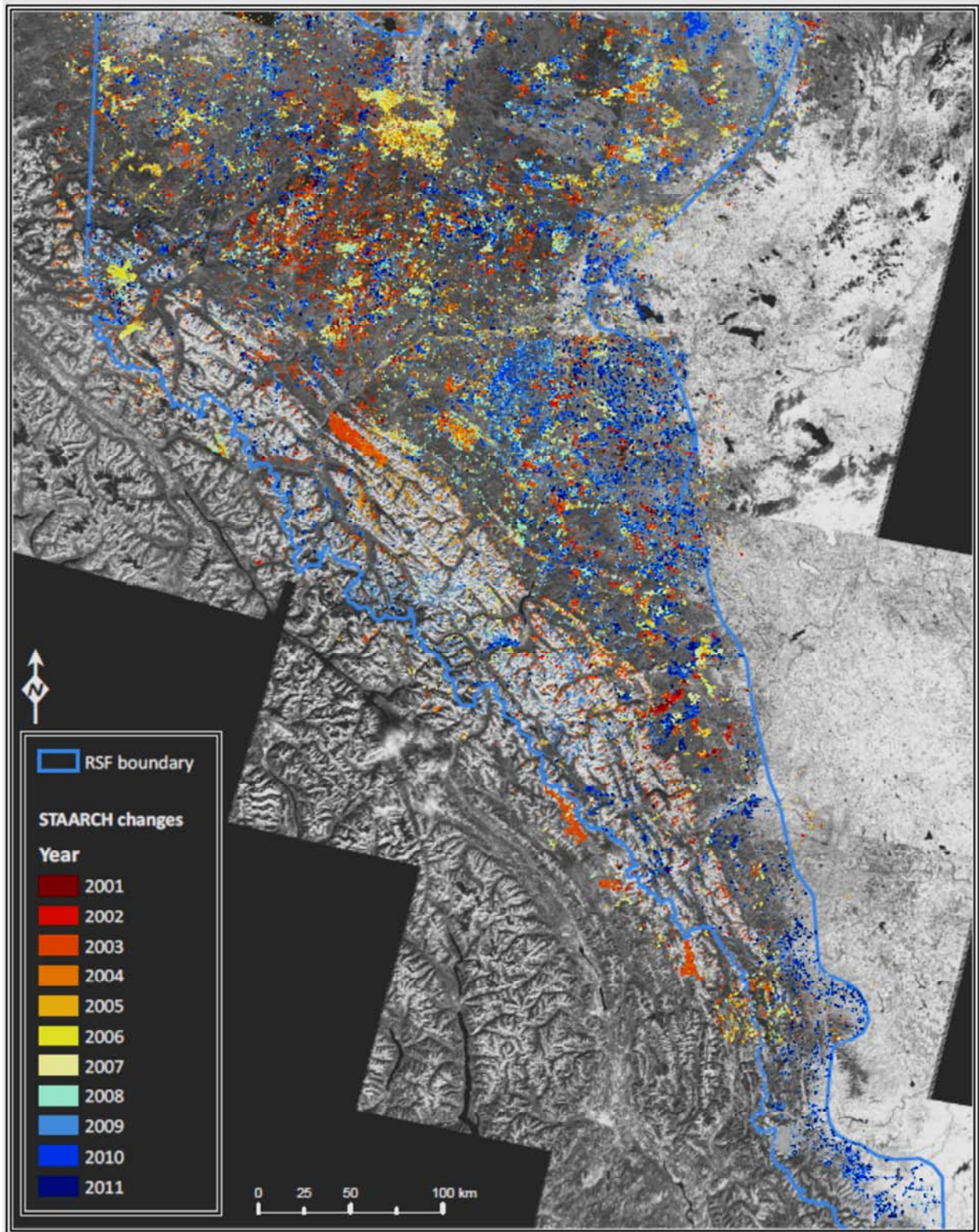


Figure 1.7 Overview of disturbances over the whole study area.

1.4 Discussion

The combined GIS layers and simulations are available as digital layers to all team participants, Alberta Innovates and Foothills Research Institute (FRI) upon request

1.5 Acknowledgements

This research was supported by Alberta Innovates, Bio Solutions. Research was undertaken by UBC researchers, Dr Thomas Hilker (now at Oregon State), Dr Wiebe Nijland (UBC Postdoc), and Mr Adam Erickson (UBC PhD Candidate).